Available online at www.sciencedirect.com

SciVerse ScienceDirect

Acta Materialia 60 (2012) 546–555

Acta MATERIALIA

www.elsevier.com/locate/actamat

Effect of a finite boundary junction mobility on the growth rate of grains in two-dimensional polycrystals

Luis A. Barrales-Mora [a,*], Günter Gottstein [a], Lasar S. Shvindlerman [a,b]

[a] Institut für Metallkunde und Metallphysik, RWTH Aachen, Kopernikusstrasse 14, D-52056 Aachen, Germany
[b] Institute of Solid State Physics, Russian Academy of Sciences, Chernogolovka, Moscow District 142432, Russia

Received 21 July 2011; received in revised form 4 October 2011; accepted 12 October 2011
Available online 22 November 2011

Abstract

The effect of a finite triple junction mobility on the growth rate of two-dimensional polycrystals is studied by means of computer simulations. The equations that describe this effect are derived on the basis of the von Neumann–Mullins equation. The derived equations are compared to network-model computer simulations and show a good agreement. An analysis of the grain growth kinetics points out that the effect of the initial topology prior to the onset of grain growth is stronger than previously thought. This indicates as well that grain growth controlled by triple junctions cannot be estimated only from the kinetics.

Keywords: Grain growth; Finite mobility of triple junctions; von Neumann–Mullins relation

1. Introduction

Grain growth occurs as a necessity of a polycrystal to minimize its free energy through the elimination of grain boundary area. The grain boundaries provide, consequently, the driving force for their own motion. Nevertheless, during grain growth other structural elements are also involved, namely triple lines and quadruple junctions. Evidently, grain growth entails the concomitant motion of all of these structural elements. Most theories on grain growth assume that triple lines and quadruple junctions do not influence the motion of the grain boundaries. However, this may not be the case, since in several recent investigations [1–5] it has been effectively shown that these elements can have kinetics different from the grain boundaries and thus, drag grain boundary motion and consequently affect grain growth. Since a polycrystal is a connected network of grain boundaries and their junctions, the elements with the slowest migration rate will govern grain growth kinetics. Slower kinetics is equivalent to a lower effective driving force. Since the driving force is reflected by grain boundary curvature, its change is accompanied by a variation of the dihedral angle θ and turning angle β ($=\pi-\theta$) at grain boundary junctions and its dependency on the mobilities of the different structural elements. Since most of the theories on grain growth assume a dihedral angle of 120° at triple junctions of two-dimensional (2-D) grain structures, they fail to predict accurately the grain growth evolution in the case of a finite mobility of the boundary junctions. There have been a few attempts in the literature to correct this. For instance, Gottstein and Shvindlerman [6] modified the von Neumann–Mullins relation to consider the effect of a finite triple line mobility. In their approach, they consider that the dihedral angle of grains with less than six grain boundaries ($n<6$) will tend to 0°, while the dihedral angle for grains with more than six grain boundaries will tend to 90° for very slow triple junction kinetics. In the present paper, this approach is first critically reviewed. Subsequently, 2-D network model simulations are performed to corroborate the theoretical model presented here.

* Corresponding author. Tel.: +49 (0) 241 8026877; fax: +49 (0) 241 8022301.
E-mail address: barrales@imm.rwth-aachen.de (L.A. Barrales-Mora).

1359-6454/$36.00 © 2011 Acta Materialia Inc. Published by Elsevier Ltd. All rights reserved.
doi:10.1016/j.actamat.2011.10.022

2. Triple junctions and a first approach to the von Neumann–Mullins relation

The study of the kinetic properties of a system with triple junctions is only possible in the course of steady-state motion. However, the steady-state motion can be achieved only in those granular arrangements whose geometry provides an independency of the driving force on time. In Fig. 1, two geometrical configurations that allow a steady-state motion of their triple junctions are shown. It is possible to derive the equations of motion for the grain boundaries and triple junctions from the geometry of these grain arrangements and thus to determine the effect of a finite triple junction mobility on the evolution of the system [5].

The influence of the triple junction is expressed by a dimensionless parameter Λ_{tj} in terms of the change of the dihedral θ and turning β angles. For the configuration shown in Fig. 1a, Λ_{tj} reads:

$$\Lambda_{tj}(a) = \frac{m_{tj}a}{m_{gb}} = \frac{\theta}{2\cos\frac{\theta}{2} - 1} = \frac{\pi - \beta}{2\cos\frac{\pi-\beta}{2} - 1} \tag{1}$$

and for the grain system shown in Fig. 1b:

$$\Lambda_{tj}(x_0) = \frac{m_{tj}x_0}{m_{gb}} = -\frac{\ln\sin(\pi-\theta)}{1-2\cos(\pi-\theta)} = -\frac{\ln\sin\beta}{1-2\cos\beta} \tag{2}$$

where m_{tj} and m_{gb} are the triple junction and grain boundary mobilities, respectively. The dimensions x_0 and a are shown in Fig. 1. It is possible to substitute x_0 in Eq. (2) by the distance a between triple junctions since the function for the shape of the grain boundary is known and given by [7]:

$$y(x) = -\frac{x_0}{\ln\sin\beta}\arccos e^{\frac{x}{x_0}\ln\sin\beta} \tag{3}$$

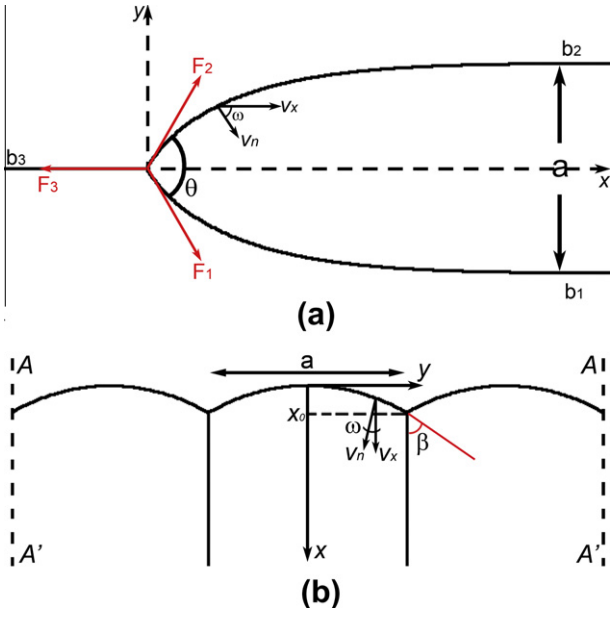

Fig. 1. Special geometrical grain arrangements that allow the steady-state motion of the grain boundaries and triple junctions.

For $x = x_0$, $y = a/2$ and by substituting these values in Eq. (3) x_0 can be expressed as a function of a and β:

$$x_0 = -\frac{a\ln\sin\beta}{2\left(\frac{\pi}{2} - \beta\right)} \tag{4}$$

Finally, substitution of Eq. (4) in Eq. (2) yields:

$$\Lambda_{tj}(a) = \frac{m_{tj}a}{m_{gb}} = \frac{2\left(\frac{\pi}{2} - \beta\right)}{1 - 2\cos\beta} = \frac{2\left(\theta - \frac{\pi}{2}\right)}{1 - 2\cos(\pi - \theta)} \tag{5}$$

It is obvious from Eqs. (1) and (5) that the triple junctions are able to drag the motion of the adjoining grain boundaries [5] upon change of the turning angle and thus of the dimensionless parameter Λ_{tj}. Since the dependency $\Lambda_{tj}(\beta)$ is known, it is possible to formulate an equation for the growth rate of grains affected by triple junction drag. The von Neumann–Mullins relationship [8] states that the area (S) rate of change of any 2-D grain is proportional to the grain boundary energy γ, mobility m_{gb} and the curvature of its grain boundaries:

$$\frac{dS}{dt} = -m_{gb}\gamma(2\pi - n\beta) \tag{6}$$

In Ref. [6], Gottstein and Shvindlerman classified the problem into two categories according to the topological class n of the grains and derived equations for the growth rate of grains with $n < 6$ and $n > 6$. For this, they used a series expansion of Eqs. (1) and (2) in the neighborhood of $\pi/3$ and solved for β to arrive at [6]:

$$\dot{S} = \frac{m_{gb}\gamma\pi}{3}\left(n\frac{6 + \sqrt{3}\Lambda_{tj}}{2 + \sqrt{3}\Lambda_{tj}} - 6\right) \quad (n < 6) \tag{7a}$$

and

$$\dot{S} = \frac{m_{gb}\gamma\pi}{3}\left[n\left(1 + \frac{6\ln\sin\pi/3}{\pi\sqrt{3}\Lambda_{tj}}\right) - 6\right] \quad (n > 6) \tag{7b}$$

As expected, these equations show good agreement for large values of Λ_{tj} [6] but cannot predict accurately the growth rate of grains with small Λ_{tj}. The good agreement for large Λ_{tj} owes to the fact that independent of the topological class the turning angle of a grain will tend to $\pi/3$ for $\Lambda_{tj} \gg 1$. In turn, the approach is bound to fail for small values of Λ_{tj} because the turning angle for $\Lambda_{tj} \to 0$ depends on the topological class n since polygonal grains will have different contact angles depending on their number of sides. This case was not considered in the derivation of Eqs. (7a) and (7b). In the following sections, we propose two different approaches that consider this dependency and seem to describe correctly the growth rate of a grain for all values of Λ_{tj}.

3. Growth rate of a grain in a polycrystal with finite mobility of the triple junctions: a polygonal approach

A finite mobility of the boundary junctions causes, during grain growth, a flattening of the grain boundaries as a necessity to reduce their driving force and allow the system

to evolve with the kinetics that guarantee the concomitant motion of all structural elements of the microstructure and, at the same time, a maximal minimization rate of the free energy. Since the configurations shown in Fig. 1 have a very particular geometry, it is possible to determine exactly the influence of the triple junctions on the curvature of the grain boundaries. However, such geometries are unlikely to be found in polycrystals and therefore their applicability is limited to very controlled experiments. To overcome this difficulty we propose the geometry of an n-sided grain shown in Fig. 2.

For the geometry shown in Fig. 2 the velocity of the triple junction can be calculated from the equilibrium of forces at the triple junctions. With the assumption that the grain boundary energy is homogeneous and constant, the net force exerted on the junction reads:

$$P = \gamma(2\cos\varphi - 1) \tag{8}$$

and correspondingly, the velocity of the triple junction is given by:

$$v_{tj} = m_{tj}\gamma(2\cos\varphi - 1) \tag{9}$$

where φ is half the dihedral angle (Fig. 2). In turn, the velocity of the grain boundary follows the fundamental equation:

$$V_{gb} = m_{gb}\gamma\kappa \tag{10}$$

where κ is the curvature of the grain boundary. Considering the grain boundaries as circular arcs the curvature can be calculated as:

$$\kappa = \frac{1}{r} = \frac{2\sin\alpha}{a} \tag{11}$$

Evidently, the curvature depends on the length a between triple junctions. It can be noticed that the parameter a has the same physical meaning as in Fig. 1, i.e. the magnitude of the driving force. In order to equate the velocities of the triple junction and the grain boundaries (necessary condition for a concomitant motion), the grain boundary velocity has to be projected onto the direction of motion of the triple junction. This projected velocity v_{gb} of the grain boundary reads:

$$v_{gb} = \frac{2m_{gb}\gamma\sin\alpha}{a}\sin\varphi \tag{12}$$

Equating both velocities leads to the parameter Λ_{tj}:

$$\Lambda_{tj} = \frac{m_{tj}a}{m_{gb}} = \frac{2\sin\alpha\sin\varphi}{2\cos\varphi - 1} \tag{13}$$

This equation can as well be expressed in terms of either the dihedral angle θ or the turning angle β. For convenience from now on, we will use only the expressions for β since this angle can be substituted directly in Eq. (6). Eq. (13) can then be rewritten as:

$$\Lambda_{tj} = \frac{m_{tj}a}{m_{gb}} = \frac{\sin\left(\frac{\pi}{n}\right) - \sin\left(\beta - \frac{\pi}{n}\right)}{2\sin\left(\frac{\beta}{2}\right) - 1} \tag{14}$$

This approach seems to be fully consistent with our understanding of grain boundary junctions in polycrystals since, as in the case for the simpler configurations shown in Fig. 1, when $\beta \to \pi/3$ $\Lambda_{tj} \to \infty$ and in turn, when the angle $\beta \to 2\pi/n$ (for flat grain boundaries) then $\Lambda_{tj} \to 0$. The first case corresponds to perfectly grain-boundary-controlled motion whereas the second relates to perfectly triple-junction-controlled motion.

In order to modify the von Neumann–Mullins relationship [8] (Eq. (6)), it is necessary to solve Eq. (14) for β. In contrast to Eqs. (1) and (2) which seem not to have an analytical solution, Eq. (14) can be solved analytically. However, the solution is very lengthy, and thus it will not be presented here. Nevertheless, in a subsequent section we will show by means of network model simulations that this approach can be used to predict the growth rate of grains with different topological classes.

For 2-D grains the von Neumann–Mullins equation can be used to calculate the growth rate of grains for ideal conditions, i.e. m_{gb} and γ are assumed constant. The von Neumann–Mullins relation predicts that the growth rate of a 2-D grain depends exclusively on the topological class. However, if ideal conditions are inexistent then the growth rate will depend as well on the turning angle, see Eq. (6). For our analysis, we need an equation for the 2-D growth rate with consideration of the finite mobility of the triple junctions. For this we need only a combination of Eq. (6) and the solution of Eq. (14) for the turning angle β.

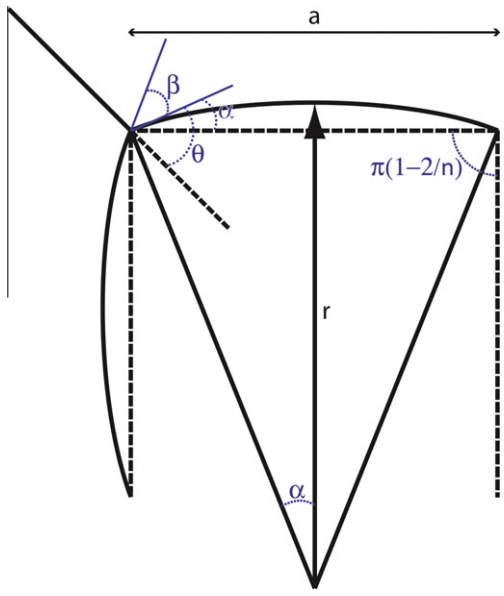

Fig. 2. Geometry of an n-sided grain used for the derivation of the equations of motion.

4. 2-D network model simulations

Various models have been used for the simulation of grain boundary migration and related phenomena, in particular grain growth and recrystallization: notably Monte Carlo [9–12], phase field [13,14] and network models [15–19]. However, models based on cellular automata [20,21],

finite elements [22], and molecular dynamics [23] can also be found in the literature. Among them, the network models stand out for the clarity of the physics used for the description of grain boundary migration. The deterministic character of these models allows an easy implementation of a finite boundary-junction mobility [18,24–26]. The implementation of the model utilized in this study is described elsewhere [18,26]. This model has been tested by simulations of diverse phenomena involving grain boundary migration [24,25] including 2-D grain growth in polycrystals with finite mobility of the boundary junctions [25]. In the following section, we will first show that the simulation model is able to correctly simulate grain growth in the configuration depicted in Fig. 1b, and then we will utilize the simulation model to study the polycrystalline case.

4.1. Steady-state and non-steady-state grain boundary motion

In order to analyze the accuracy of the model, we reproduced the geometry of the grain arrangement shown in Fig. 1b in computer simulations (Fig. 3). In these simulations the grain boundary energy and mobility were kept constant whereas the triple junction mobility was varied in order to establish different kinetic regimes. The turning angle β, area, and growth rate of the central grain (grain 1 in Fig. 3) were recorded during the whole simulation.

The accuracy of the turning angle can be easily determined because Eq. (5) is the exact solution for the parameter Λ_{tj} as a function of β and a. Since a is constant the effect of Λ_{tj} can be singled out. As expected, the grain boundaries tend to flatten for decreasing Λ_{tj}; a comparison of Eq. (5) with the mean value of the angle recorded during the simulation renders excellent agreement (Fig. 4). Large deviations of the measured values observed for $\Lambda_{tj} \gg 1$ can be explained by the fact that the angles shown in Fig. 4 correspond to the mean value, which includes as well the values of the turning angle during and before relaxation. Evidently, the turning angle of the starting configuration ($\pi/2$) is further away from the equilibrium angles for $\Lambda_{tj} > 1$ than from the turning angles for $\Lambda_{tj} < 1$.

More important is to determine the accuracy of the growth rate of the central grain in Fig. 3 since this parameter will be used for analysis of the polycrystal simulations. In Fig. 3 any grain of the arrangement corresponds to a four-sided grain with an open boundary on the right side; for this reason, the growth rate of any grain can be calculated by applying Eq. (6) as follows:

$$\dot{S}_G = \frac{-m_{gb}\gamma}{2}(2\pi - 4\beta) = m_{gb}\gamma(2\beta - \pi) \tag{15}$$

The only unknown variable in this equation is the turning angle β but it can be numerically calculated for any Λ_{tj} using Eqs. (5) and substituted into Eqs. (15) and (16). Consequently, the area S of a grain varies as function of time as:

$$S = S_0 + m_{gb}\gamma(2\beta - \pi) \cdot t \tag{16}$$

where S_0 is the initial area, and t is the time. In Fig. 5 the simulated area change with time is compared to the one calculated with Eqs. (16) and (5) for different values of Λ_{tj} corresponding to the three different kinetic regimes, i.e. grain boundary kinetics ($\Lambda_{tj} \gg 1$), transition kinetics ($\Lambda_{tj} \approx 1$) and triple junction kinetics ($\Lambda_{tj} \ll 1$). Despite some minor deviations, good agreement can be observed for different values of Λ_{tj} in the three regimes. A more comprehensive comparison can be seen in Fig. 6, where Eq. (15) is plotted along with the simulation results for the growth rate of the central grain in Fig. 3 in dependency of Λ_{tj}.

From the previous results it is obvious that the simulation model can predict correctly the behavior of a grain assembly evolving in steady state and under the influence of a finite mobility of the triple junctions. However, it is not clear whether the model or the approaches described in the previous sections can reproduce the features of grain growth since in this phenomenon, the driving force is not constant and therefore the grains do not evolve in steady state. To evaluate the simulation model and the various

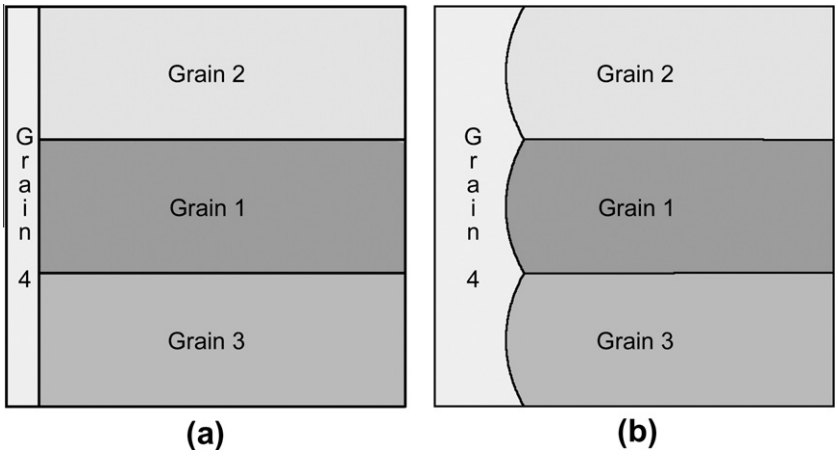

Fig. 3. (a) Grain configuration used for the simulations of the configuration shown in Fig. 1b at time t_0 and (b) after relaxation, when steady-state motion occurs.

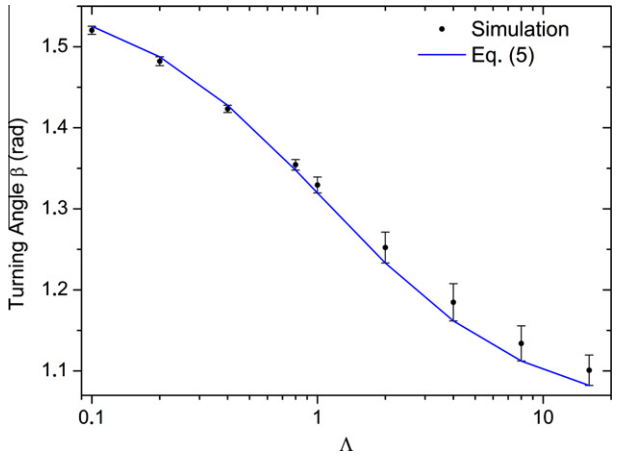

Fig. 4. Turning angle as a function of the parameter Λ_{tj}.

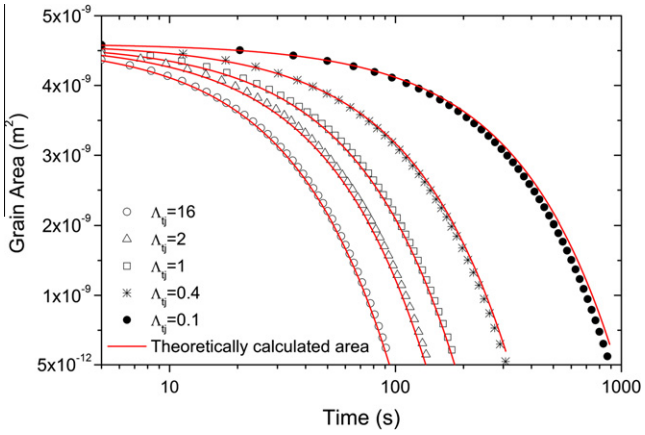

Fig. 5. Comparison of the simulation results for the central grain of the configuration shown in Fig. 3 with Eq. (16). The data are shown in logarithmic time units for better visibility. The necessary turning angle β for the calculation of the growth rate was determined by numerically solving Eq. (5) for the different values of Λ_{tj}.

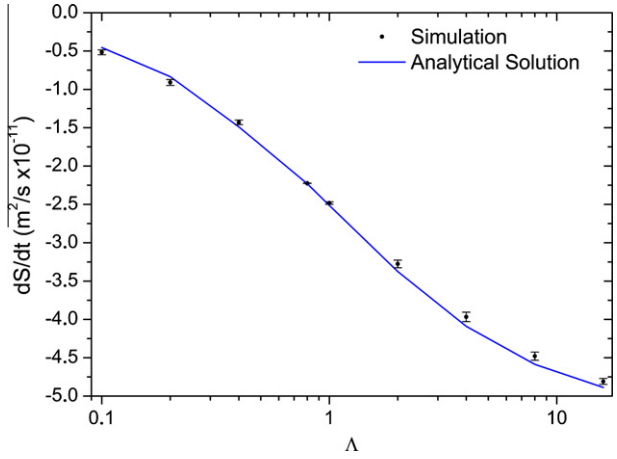

Fig. 6. Comparison of the simulated growth rate of the central grain in Fig. 6 with the analytically calculated rate (Eq. (15)).

introduced approaches, we carried out simple simulations using a four-sided grain, as depicted in Fig. 7, under the influence of a finite triple junction mobility. The results for the growth rate of the grain were compared with the original (Eq. (7a)) and polygonal (Eq. (14)) approaches for the prediction of the growth rate.

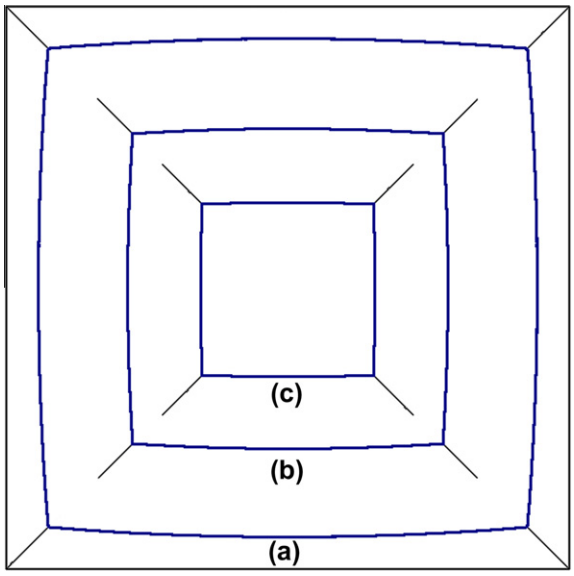

Fig. 7. Four-sided grain used to validate the polygonal approach. Since the size of the grain decreases with time, Λ_{tj} changes as well. For this reason, the grain boundaries of the grain experience a flattening with decreasing grain size. Evidently, the grain boundaries of the grain in (a) are more prominently curved than the grain boundaries in (b and c).

The shape of a four-sided grain after different simulation times is depicted in Fig. 7. It can be noticed that the dihedral angle at the triple junctions decreases with decreasing grain size. This occurs because Λ_{tj} decreases linearly with grain size (through the distance between vertices a in Eq. (14)) and thus affects dynamically the evolution of the grain. The system has, therefore, to adapt its driving force by flattening the grain boundaries due to the kinetic constraints imposed by the triple junctions.

Since the grain size decreases continually, it is possible to evaluate with one simulation the whole interval of Λ_{tj}. Evidently, the growth rate of the grain depends on time as the finite triple junction mobility influences the kinetic equilibrium of the grain surface. Nevertheless, the growth rate can be evaluated independently of time if only its dependency of Λ_{tj} is considered. In Fig. 8 the growth rates obtained from the simulations (open circles) are compared to the different predictions. Notably, the polygonal approach delivers the best agreement with the simulations. The original approach agrees with the simulations only for $\Lambda_{tj} \gg 1$, as expected from its respective assumptions.

4.2. Polycrystal simulations

Since the simulation model predicts accurately the growth rate of grains in simple simulation setups it qualifies for a simulation of polycrystals with consideration of a finite triple junction mobility. Since the grain size increases with time, it is possible to evaluate a range of Λ_{tj} depending

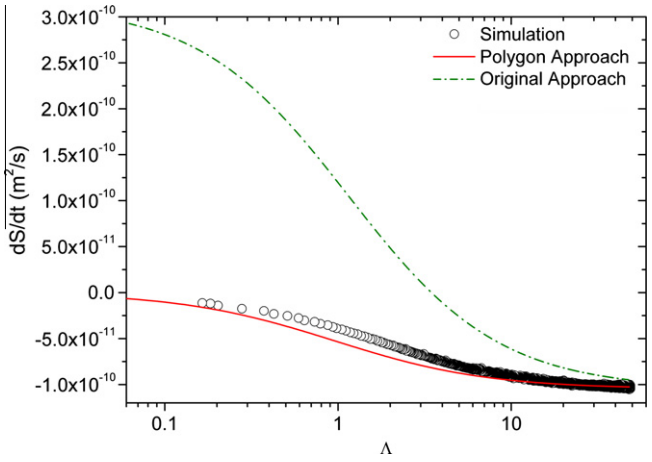

Fig. 8. Comparison of the different approaches with the growth rate of the four-sided grain shown in the figure. The polygonal approach shows a good agreement for the whole interval of Λ_{tj}, whereas the original equation shows good agreement only for $\Lambda_{tj} \gg 1$.

on the initial grain size and/or triple junction mobility. In order to cover a broad range of Λ_{tj}, three simulations were carried out with different initial triple junction mobilities. All other simulation parameters (γ, m_{gb}) were kept constant for all tests. As the grains change their size constantly and therefore alter the value of Λ_{tj}, it was necessary to keep continuous track of their geometrical properties, growth rate and Λ_{tj}. The parameter a for the calculation of Λ_{tj} was taken as the mean distance between vertices of a grain (Eqs. (1) and (14)). Experimentally, a can be extracted from the grain size through the perimeter p since $a \approx p/n$ for the calculation of Λ_{tj}. This was not necessary in these simulations as all the required geometrical information was available.

The results of the simulations are summarized in Figs. 9 and 10 for grains with $n \leqslant 6$ and $n > 6$, respectively. The respective growth rates of grains for a specific topological class are compared to the previously introduced theoretical predictions for changing Λ_{tj}. As in the simulation of the four-sided grain, in general, the polygonal approach seems to predict the growth rate of 2-D grains reasonably well. The original approach matches the simulations for $\Lambda_{tj} \gg 1$ according to its setup.

The growth rates for grains with $n = 6$ (Fig. 9d) represent a special case since both the original and the polygonal approaches assume a zero growth rate for grains within this class. This assumption is based on the false premise that six-sided grains have straight grain boundaries and thus they are not affected by a finite triple junction mobility. For the polygonal approach, there is no alternative since the grains are assumed to be regular polygons with curved faces, in which case the six-sided grain will have straight grain boundaries. However, in reality, once a six-sided grain assumes an irregular non-equiangular shape the grain boundaries have to become curved in order to establish the equilibrium at the triple junctions. If the triple junctions additionally promote a flattening of the grain boundaries then most of the non-equiangular six-sided grains will shrink since dihedral angles larger than 120° (a dihedral angle larger than 180° is physically impossible for isotropic γ) contribute only marginally to the growth of the grains whereas dihedral angles smaller than 120° induce a rapid shrinking of the grain in order to attain equilibrium at the triple junctions. Fig. 9d substantiates that most of the measurements for $n = 6$ lie below the zero growth rate line.

We can conclude that for a hypothetical purely triple-junction-controlled grain growth (i.e. perfectly flat grain boundaries), the condition for zero growth will depend not only on the topological class ($n = 6$) but also on the shape of the grain since only hexagonal equiangular grains have dihedral angles equal to 120°. In general, the von Neumann–Mullins equation (Eq. (6)) predicts that any grain that fulfills $\beta = 2\pi/n$ will have a zero growth rate, a condition which is met by equiangular polygons. Nevertheless, even if the grains can assume this shape, they cannot have a zero growth rate unless they are hexagonal and equiangular because the grain boundaries of grains with $n \neq 6$ will have contact angles different from 120°, and this will ultimately drive their motion. For practical purposes, it can be said that for purely triple-junction-controlled grain growth there is not a unique topological class with zero growth rate since it is very unlikely that all six-sided grains in a real microstructure are equiangular. Furthermore, any topological transformation of an adjacent grain boundary at the triple junction will disrupt the instant equilibrium. However, this imposes an additional constraint to the growth of grains in polycrystals because an equiangular hexagonal grain cannot grow at all as it experiences no driving force. This constraint is removed for zero triple-junction-drag since in this case the triple junctions and grain boundaries of a six-sided grain might experience a driving force and move. This is an apparent contradiction with the von Neumann–Mullins equation but it has to be noted that this equation explicitly states that the growth rate of grains does not depend on its shape, which means that the shape of six-sided grains can and in fact do change during their evolution while satisfying a zero growth rate. This eases the occurrence of topological transformations, which are unlikely to occur smoothly in grain growth controlled exclusively by triple junctions, because equiangular hexagonal grains are completely static and can evolve only through topological interactions with neighboring grains.

The results for grains of topological classes $n > 6$ (Fig. 10) only confirm the good agreement of the polygonal approach with the simulation results. An important conclusion from this analysis is that the growth rate of grains with finite mobility of the triple junctions depends on the shape of the grain since grains with the same Λ_{tj} can have different growth rates.

4.3. Grain growth kinetics

It is tacitly believed that triple-junction-controlled grain growth is characterized by a parabolic change of the grain

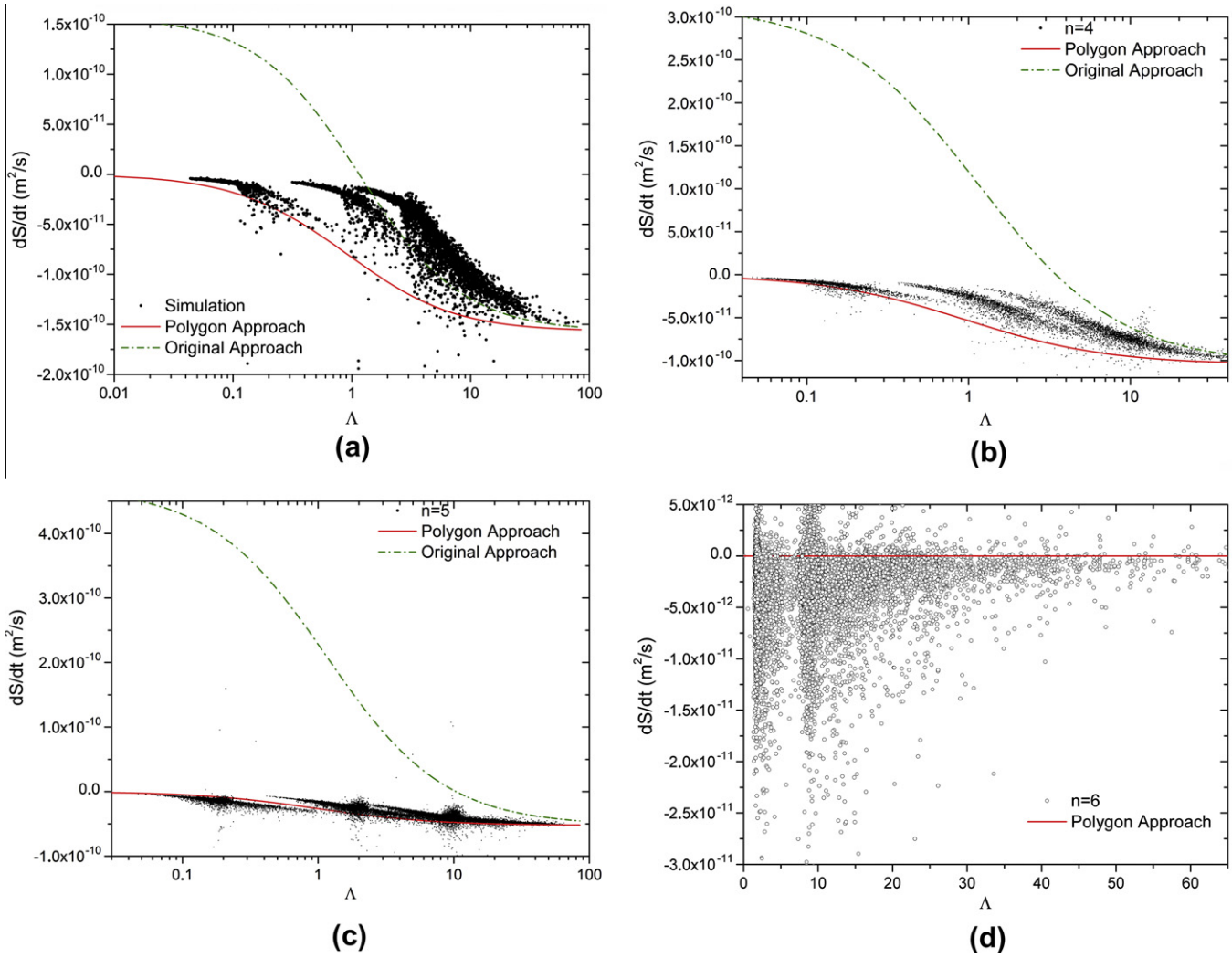

Fig. 9. Comparison of the simulated growth rate for grains with $n \leqslant 6$ and the theoretical approaches. A good agreement of the polygonal approach can be observed. The dots correspond to three simulations with different starting triple junction mobility to achieve a broad range of Λ_{tj}. For $n = 3$ (a) the original approach shows a good agreement for $\Lambda_{tj} \geqslant 1$; for (b) $n = 4$ and (c) $n = 5$ the polygonal approach seems to agree better with the simulation. In (d) the growth rate for grains with $n = 6$ shows that these grains tend to shrink in the case of a low Λ_{tj}.

area S with time: $S \sim t^2$, in contrast to boundary-controlled grain growth: $S \sim t$. Whereas parabolic kinetics have been confirmed by computer simulations of 2- and 3-D triple-junction-controlled grain growth with the Monte Carlo–Potts model [27,28], in network model simulations a growth exponent of $m = 1.75$ has been typically found [29], which clearly deviates from the $m = 1$ expected for grain-boundary-controlled grain growth. Triple junction kinetics are particularly expected in nanocrystalline materials because more polycrystal volume is occupied by triple junctions (topologically the most frequent structural element) and very small values of Λ_{tj} can be achieved as the distance between junctions decreases in proportion to the grain size [30]. However, we will show that the determination of triple junction kinetics may not be as simple as previously thought because the topology of the sample might play a more dominant role during grain growth.

The average 2-D grain area undergoing ideal grain growth follows linear kinetics. This is basically a result of the topological constraints imposed on the polycrystal [31–33] that force the conservation of a self-similar grain size distribution. Self-similarity, however, can only be attained in steady state, but not during the transient from non-equilibrium structures [27,28]. Whereas the equilibrium distributions for triple-junction-affected grain growth have been recently theoretically determined [28] and validated by means of computer simulations [27], it still remains an open question, how a finite triple junction mobility can affect the attainment of a steady-state microstructural development. In order to elucidate this issue, we performed simulations of grain growth under different conditions: from curvature-controlled to triple-junction-controlled grain growth.

In Fig. 11, the grain growth kinetics for different triple junction mobilities are plotted. The curves are fitted to the function $\langle S(t) \rangle - \langle S(0) \rangle = kt^m$, where $\langle S \rangle$ is the mean grain area, k is the kinetic constant and m is the grain growth exponent. The effect of the triple junction mobility

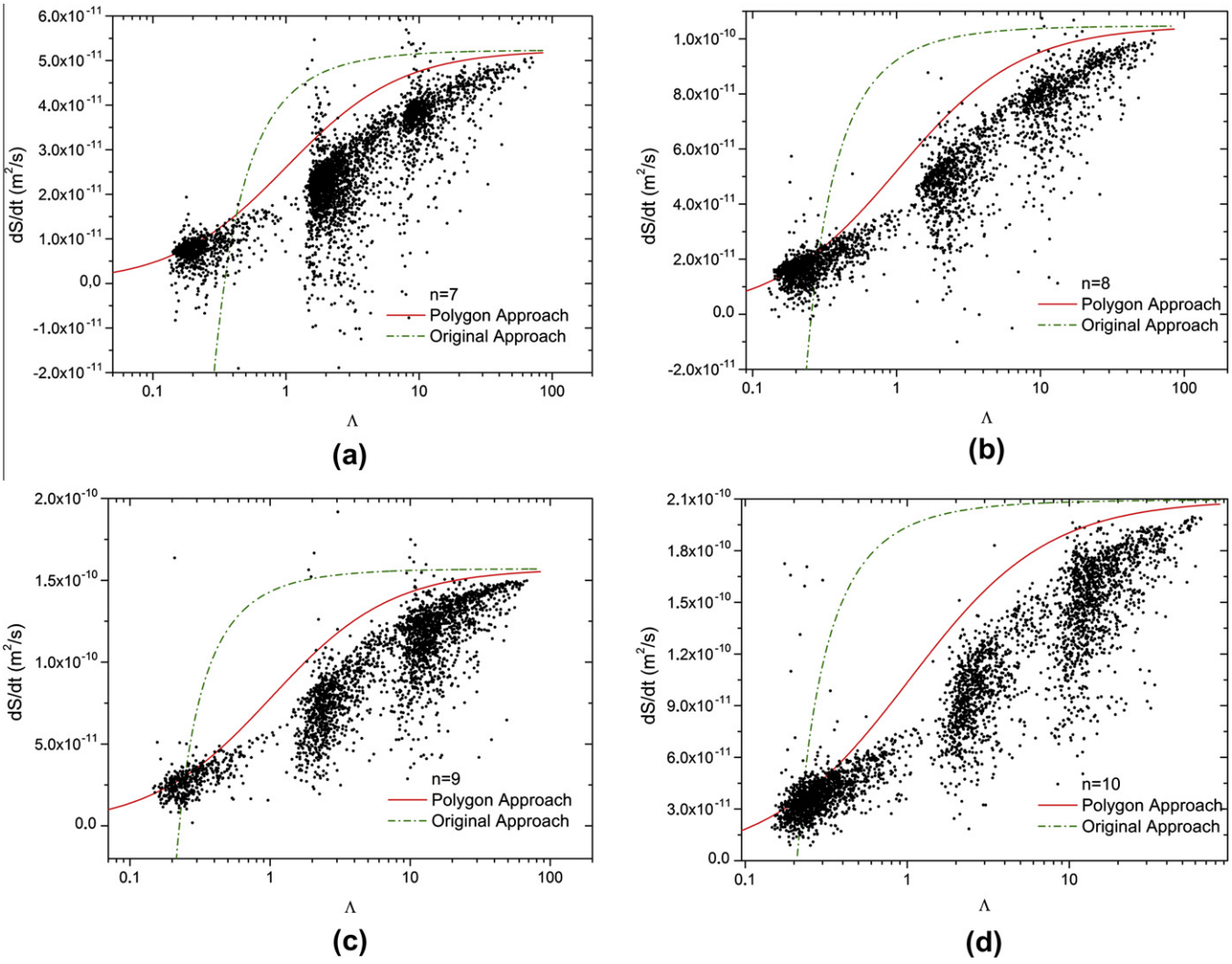

Fig. 10. Comparison of the theoretical approaches and the simulated growth rate for grains of the topological class (a) $n = 7$, (b) $n = 8$, (c) $n = 9$ and (d) $n = 10$.

on grain growth kinetics is expressed by the grain growth exponent that tends to unity for increasing triple junction mobility. It is noted that the values for m are lower than the grain growth exponent found by Weygand et al. [29] ($m \approx 1.75$), who simulated grain growth controlled exclusively by the triple junctions. For their simulations, they considered straight grain boundaries and calculated the velocity of the triple junctions simply from the product of the triple junction mobility and the net grain boundary surface tension at the junction. This approach seems to represent an upper limit for triple junction kinetics as the grain boundaries are completely flat and do not contribute to the minimization of the free energy. They also reported that after some time their simulation structures attained self-similarity and thus followed linear kinetics. This has been confirmed by other authors [27,28,34,35] as well. Since even in the case of purely triple-junction-controlled grain growth self-similarity and linear kinetics are promptly achieved, the effect of the triple junctions is apparently reflected only

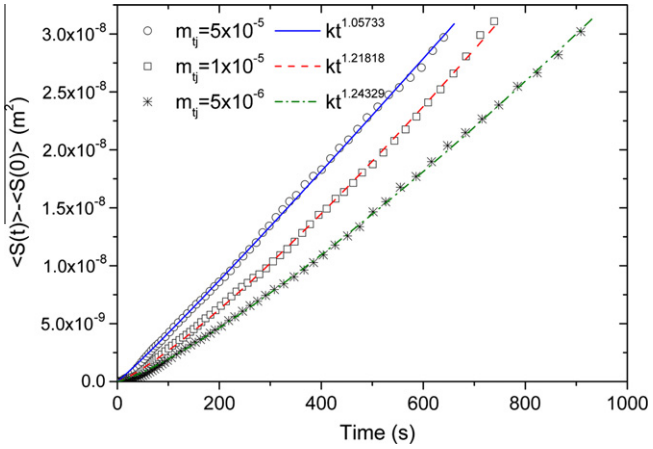

Fig. 11. Grain growth kinetics for different starting finite triple junction mobilities (m_{tj} in $m^3\,J^{-1}\,s^{-1}$). An increase of the triple junction mobility results in a quick convergence to linear kinetics.

during the transient phase of grain growth. Such transient has been reported in several grain growth simulations, including ideal grain growth [35–37], and is apparently caused by an initial non-equilibrium grain size distribution. For instance, Fig. 12 (initial Voronoi tessellation) shows that the grain growth exponent m even for ideal grain growth can strongly deviate from unity if the initial grain size distribution is not in equilibrium. Note that for that simulation the triple junction mobility was considered infinite.

The effect of the initial distribution on the kinetics of purely triple-junction-controlled grain growth is shown in Fig. 13. Two simulations with different initial grain size distributions are represented. Open triangles correspond to a distribution as obtained from a Voronoi tessellation, whereas the data represented by open circles correspond to a microstructure obtained from ideal grain growth simulations after self-similarity was attained. The other simulation parameters were identical for both cases. The grain growth exponent for the former simulation case was $m = 1.7$, similar to the exponent reported in Ref. [29] for simulations with an initial Voronoi network. By contrast, for the latter case, the exponent was equal to $m = 1.45$. These results substantiate that for the same physical conditions the topology of the sample can impact the kinetics. An important conclusion from this analysis is that, while triple junctions indeed influence the kinetics of grain growth, the magnitude of this effect depends on the topology as well. In other words, the effect of the triple junctions cannot be extracted from only the kinetics as they are influenced by both physical (triple junction drag) and topological (space filling) constraints. In a more general sense, this analysis proves that identifying the particular effect of some physical constraint from only the kinetics is not adequate as the initial topological state of the sample might have a larger influence. Furthermore, it is noted that contrary to expectations parabolic kinetics ($S \sim t^2$) were not achieved in the simulations for triple-junction-controlled grain growth. This result suggests that microstructural development under these conditions is still affected by a microstructural dimension (whether this is the grain size or another parameter is still an open question) like in grain-boundary-controlled grain growth where the driving force scales with the reciprocal average grain size. This will be an issue of future research.

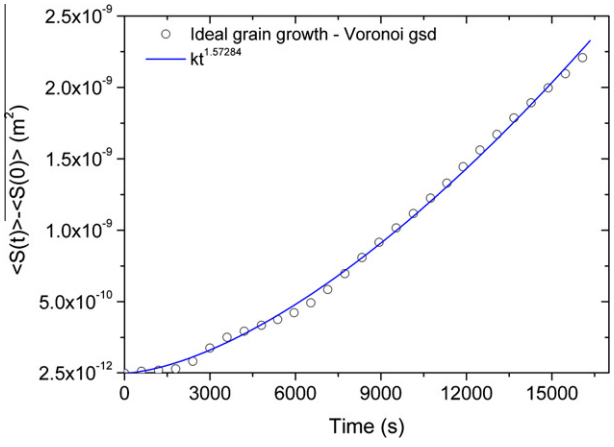

Fig. 12. Ideal grain growth simulation with a starting Voronoi mosaic as input. Since the grain size distribution is not in equilibrium, the kinetics does not obey linearity. Once the distribution is equilibrated, the kinetics evolves linearly [33].

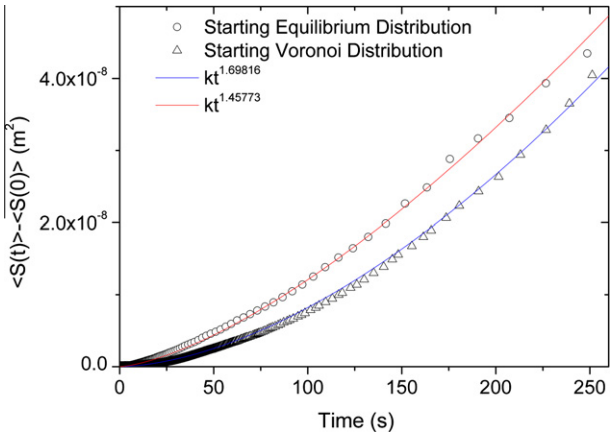

Fig. 13. Triple-junction-controlled grain growth. The different kinetics result from the difference in the starting grain size distribution. For the open triangles a Voronoi mosaic with a very narrow grain size distribution was used whereas for the open circles the equilibrium distribution as obtained from ideal grain growth simulations was utilized.

5. Conclusions

Equations for the prediction of the growth rate of 2-D grains undergoing grain growth affected by a finite triple junction mobility were derived. They were shown to accurately predict the growth rates for a large range of triple junction mobilities and showed good agreement with network-model simulations. An analysis of the grain growth kinetics points out that the effect of the initial topology prior to grain growth is stronger than previously thought. This indicates as well that the strength of triple junction effects on grain growth cannot be derived from grain growth kinetics only.

Acknowledgements

Financial assistance from the collaborative research center of the Deutsche Forschungsgemeinschaft (DFG) SFB 761 “Stahl *ab-initio*” and through project Go335 of the DFG is gratefully acknowledged. We appreciate the financial support of the cooperation through the DFG Grant RUS113/846/0-2(R) and the Russian Foundation of Fundamental Research (Grant DFG-RRFI 09-02-91339).

References

[1] Gottstein G, Shvindlerman LS. Scripta Mater 2006;54:1065.
[2] Ivanov VA, Molodov DA, Shvindlerman LS, Gottstein G. Acta Mater 2004;52:969.

[3] Protasova SG, Gottstein G, Molodov DA, Sursaeva VG, Shvindlerman LS. Acta Mater 2001;49:2519.
[4] Barrales Mora LA, Mohles V, Shvindlerman LS, Gottstein G. Acta Mater 2008;56:1151.
[5] Czubayko U, Sursaeva VG, Gottstein G, Shvindlerman LS. Acta Mater 1998;46:5863.
[6] Gottstein G, Ma Y, Shvindlerman LS. Acta Mater 2005;53:1535.
[7] Gottstein G, Shvindlerman LS. Grain interface migration in metals: thermodynamic, kinetics, applications. 2nd ed. Boca Raton, FL: CRC Press; 1999.
[8] Mullins WW. J Appl Phys 1956;27:900.
[9] Anderson MP, Grest GS, Sahni PS, Srolovitz DJ. Acta Metall 1984;32:783.
[10] Yang Z, Sista S, Elemr JW, DebRoy T. Acta Mater 2000;48:4813.
[11] Anderson MP, Grest GS, Doherty RD, Li Kang, Srolovitz DJ. Scripta Met 1989;23:753.
[12] Streitenberger P, Zöllner D. Scripta Mater 2006;55:461.
[13] Chen LQ. Scripta Met Mater 1995;32:115.
[14] Kim SG, Kim DI, Kim WT, Park YB. Phys Rev E 2006;74:061605.
[15] Kawasaki K, Nagai T, Nakashima K. Philos Mag B 1989;60:399.
[16] Maurice CL, Humphreys FJ. Thermomechanical processing in theory, modelling and practice [TMP]. Materials Park, OH: ASM International; 1997. p. 201.
[17] Weygand D, Bréchet Y, Lepinoux J. Philos Mag B 1998;78:329.
[18] Barrales Mora LA. 2D and 3D grain growth modelling and simulation. PhD thesis, Cuvillier-Verlag, Goettingen; 2008.
[19] Weaire D, Kermode JP. Philos Mag B 1983;48:245.
[20] Janssens KGF. Modell Simul Mater Sci Eng 2003;11:157.
[21] Liu Y, Baudin T, Penelle R. Scripta Mater 1996;34:1679.
[22] Kuprat A, George D, Straub G, Demirel MC. Comput Mater Sci 2003;28:199.
[23] Haslam AJ, Phillpot SR, Wolf D, Moldovan D, Gleiter H. Mater Sci Eng A 2001;318:293.
[24] Barrales Mora LA, Gottstein G, Shvindlerman LS. Acta Mater 2008;56:5915.
[25] Barrales Mora LA. Math Comp Simul 2010;80:1411.
[26] Barrales Mora La, Mohles V, Gottstein G, Shvindlerman LS. Network and vertex models for grain growth. In: Furrer DU, Semiatin SL, editors. Fundamentals of modeling for metals processing, ASM handbook, vol. 22. Materials Park, OH: ASM International; 2009.
[27] Zöllner D. Comput Mater Sci 2011;50:2712.
[28] Streitenberger P, Zöllner D. Acta Mater 2011;59:4235.
[29] Weygand D, Bréchet Y, Lépinoux J. Interf Sci 1999;7:285.
[30] Ames M, Markmann J, Karos R, Michels A, Tschöpe A, Birringer R. Acta Mater 2008;56:4255.
[31] Rivier N, Lissowski A. J Phys A: Math Gen 1982;15:L143.
[32] Rivier N. Philos Mag B 1985;52:795.
[33] Chakraverty BK. J Phys Chem Solids 1967;28:2401.
[34] Soares A, Ferro AC, Fortes MA. Scripta Met 1985;19:1491.
[35] Maurice Cl. Numerical modelling of grain growth: current status. In: Gottstein G, Molodov DA, editors. Proceedings of the first joint international conference on recrystallization and grain growth, vol. 1. Aachen: Springer Verlag; 2001. p. 123.
[36] Holm EA, Foiles SM. Science 2010;328:1138.
[37] Benson WE, Wert JA. Acta Mater 1998;46:5323.